

Competing interactions and symmetry breaking in the Hubbard-Holstein model

JOHANNES BAUER

Max-Planck Institute for Solid State Research, Heisenbergstr.1, 70569 Stuttgart, Germany

PACS 71.30.+h – Metal-insulator transitions and other electronic transitions

PACS 71.38.-k – Polarons and electron-phonon interactions

PACS 71.45.Lr – Charge-density-wave systems

PACS 71.20.Tx – Fullerenes and related materials; intercalation compounds

Abstract. - Competing interactions are often responsible for intriguing phase diagrams in correlated electron systems. Here we analyze the competition of instantaneous short range Coulomb interaction U with the retarded electron-electron interaction induced by an electron-phonon coupling g as described by the Hubbard-Holstein model. The ground state phase diagram of this model in the limit of large dimensions at half filling is established. The study is based on dynamical mean field theory combined with the numerical renormalization group. Depending on U , g , and the phonon frequency ω_0 , the ground state is antiferromagnetically (AFM) or charge ordered (CO). We find quantum phase transitions from the AFM to CO state to occur when $U - \lambda \simeq 0$, where λ characterizes the phonon induced effective attraction. The transition is continuous for small couplings and large phonon frequencies ω_0 and becomes discontinuous for large couplings and small values of ω_0 . We comment on the possible relevance of this work for $\text{Ba}_{1-x}\text{K}_x\text{BiO}_3$.

Introduction. – A classical problem in condensed matter physics is that of the competing effects of the Coulomb repulsion of the electrons with the attraction generated by the electron-phonon coupling. This appears most prominently in the theory of conventional superconductivity. There, the relatively weak attraction mediated by the phonons wins against the Coulomb repulsion with the help of retardation effects and the fact that the latter is renormalized to a reduced value at the phonon scale [1]. Only with this pseudo potential effect phonon induced superconductivity is credible in spite of the omnipresent Coulomb repulsion. Beyond such weak coupling arguments the competition of instantaneous repulsion and retarded attraction has only started to be explored in recent years with the advent of reliable strong coupling methods. In many materials the low energy physics is dominated by different competing - often strong - interactions, which need to be studied simultaneously. For example consider strongly correlated systems such as the high T_c cuprates [2], fullerenes [3], manganites [4], and organic salts [5] and their intriguing phase diagrams. The purpose of this letter is to analyze the competition of instantaneous local Coulomb repulsion and the attraction mediated by phonons for different coupling strengths, and establish the

resulting ground states, allowing for symmetry breaking in the magnetic and charge channel.

As concrete model to study the competing effects we choose the combination the fundamental model of local electronic correlations, the Hubbard model [6], with a classical model of electron-phonon coupling, the Holstein model [7]. Both models are probably oversimplified as to describe real materials in detail, but they can serve to obtain insights into dominant interaction effects. The combined Hubbard-Holstein (HH) Hamiltonian reads

$$H = -t \sum_{i,j,\sigma} (c_{i,\sigma}^\dagger c_{j,\sigma} + \text{h.c.}) + U \sum_i \hat{n}_{i,\uparrow} \hat{n}_{i,\downarrow} \quad (1)$$

$$+ \omega_0 \sum_i b_i^\dagger b_i + g \sum_i (b_i + b_i^\dagger) \left(\sum_\sigma \hat{n}_{i,\sigma} - 1 \right).$$

$c_{i,\sigma}^\dagger$ creates an electron at lattice site i with spin σ , and b_i^\dagger a phonon with oscillator frequency ω_0 , $\hat{n}_{i,\sigma} = c_{i,\sigma}^\dagger c_{i,\sigma}$. The electrons interact locally with strength U , and their density couples to an optical phonon mode with coupling constant g . Depending on U , g , ω_0 , and the filling factor n , the model is expected to display a variety of different phases including polaronic normal (N) state behavior, antiferromagnetic (AFM), charge (CO) and superconducting

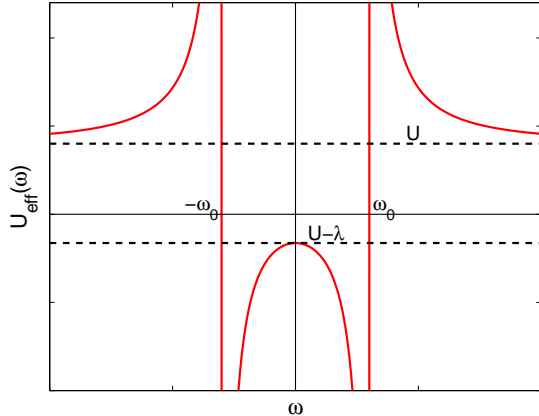


Fig. 1: (Color online) The dynamic effective interaction $U_{\text{eff}}(\omega)$ as a function of ω .

(SC) order. It is important to map out these phases to see whether for a certain material an effective description in terms of the fundamental HH Hamiltonian is sensible. We focus on the case $n = 1$.

Due to the large number of coupled degrees of freedom no exact solution of the HH model is available for the general case, and there are few analytical methods which respect the quantum nature of the phonons and allow for arbitrary coupling strengths U, g . For the pure electron-phonon problem perturbative schemes, such as Migdal-Eliashberg theory, can be very successful; strong Coulomb interactions can however not be treated. For the combined HH model there has been a lot of progress in recent years in one and infinite dimensions. In the $d = 1$ situation numerical methods can be applied with high accuracy and the phase diagram could be established [8–11]. To our knowledge for $d > 1$ general phase diagrams are still missing. In the case of high dimensions the dynamical mean field theory (DMFT) [12] becomes exact, and it can generate non-perturbative solutions, such that it becomes the method of choice for our purpose of studying arbitrary coupling strengths.

The competition of the interactions can be seen in concise form when integrating out the bosonic field, which yields an effective electronic interaction

$$U_{\text{eff}}(\omega) = U + \frac{2g^2\omega_0}{\omega^2 - \omega_0^2}. \quad (2)$$

As depicted in Fig. 1 for large ω the Coulomb repulsion U is dominant, ω_0 enters as a relevant energy scale at lower energy, and for $|\omega| \leq \omega_0$ the competition between the bare interactions is most important.

The DMFT calculations deal with these competing interactions, and as a main result of this paper the ground state phase diagram of the infinite dimensional HH model at half filling emerges. This is likely to be good approximation for the three dimensional case, where collective excitations are not dominant. As shown in Fig. 2, the transition from an AFM state to a CO state occurs near¹ $U_{\text{eff}} = 0$, where

¹For the given parameters, there is a small tendency towards

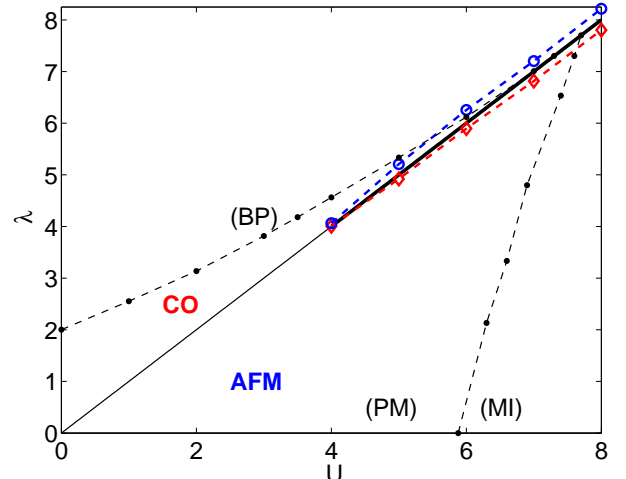


Fig. 2: (Color online) The phase diagram of AFM and CO in the U - λ -plane exemplary for $\omega_0 = 0.6t$. The thin black line $\lambda \simeq U$ gives a continuous transition and the thick line a discontinuous one. A nonzero CO/AFM order parameter was found above/below the dashed line with diamonds/circles. The dashed lines with points gives the transition for phases with no long range order, a paramagnetic metallic (PM), bipolaronic (BP) and Mott insulator (MI).

$U_{\text{eff}} = U - \lambda$ with $\lambda = 2g^2/\omega_0$. For $U_{\text{eff}} < 0$ we find a CO and for $U_{\text{eff}} > 0$ an AFM ground state. The phase boundaries for the phases without long range order, the paramagnetic metal (PM), the Mott insulator (MI), and the bipolaron (BP) insulator, are also shown in Fig. 2. We see that only for large couplings the phase boundaries merge, but for smaller couplings other scales are important as analyzed earlier for $\omega_0 = 0.2$ [13–15]. The deceptively simple result for the phase boundary of the ground state phase diagram is expected in limiting cases, such as the antiadiabatic one, $\omega_0 \rightarrow \infty$ with λ kept fixed, where as seen from (2) the HH model reduces to the Hubbard model with coupling constant U_{eff} . For the general case it is not a priori clear that this applies, as this depends on the mutual renormalization effects of the couplings at low energy. However, our results indicate that this remains valid for general ω_0 . In contrast to this universality the details and order of the transition depend on both, the couplings and the value of ω_0 .

The infinite dimensional HH model has received considerable attention and has been studied by DMFT. For instance, the formation of polarons [16] and the competition between the Coulomb repulsion and the induced interaction [17] were studied in the symmetric phase. Recently, the phase diagram of PM, BP and MI was established [13, 14], where phases with long-range order were not allowed for. Allowing for AFM order, the effect of the Coulomb repulsion on the electron-phonon interaction was investigated [18]. Here we extend these earlier calculations allowing for commensurate AFM *and* CO and

$\lambda > U$ for the transition line, which can however hardly be resolved in the plot.

establish the full ground state phase diagram. In our calculations we also studied SC solutions, but we found that for finite ω_0 CO has lower energy at half filling, thus SC does not appear in the phase diagram.

Formalism. – For our calculations we assume a bipartite lattice with A and B sublattice, where the matrix Green's function can be written in the form

$$\underline{G}_{\mathbf{k},\sigma}(\omega) = \frac{1}{\zeta_{A,\sigma}(\omega)\zeta_{B,\sigma}(\omega) - \varepsilon_{\mathbf{k}}^2} \begin{pmatrix} \zeta_{B,\sigma}(\omega) & \varepsilon_{\mathbf{k}} \\ \varepsilon_{\mathbf{k}} & \zeta_{A,\sigma}(\omega) \end{pmatrix}, \quad (3)$$

with $\zeta_{\alpha,\sigma}(\omega) = \omega + \mu_{\alpha,\sigma} - \Sigma_{\alpha,\sigma}(\omega)$, $\alpha = A, B$, and \mathbf{k} -independent self-energy [19]. For commensurate charge order, we have $\mu_{A,\sigma} = \mu - h_c$, $\mu_{B,\sigma} = \mu + h_c$ and $\Sigma_{B,\sigma}(\omega) = U n - \Sigma_{A,\sigma}(-\omega)^*$, with $n = (n_A + n_B)/2$, $n_\alpha = \sum_\sigma n_{\alpha,\sigma}$, where $n_{\alpha,\sigma} = \langle \hat{n}_{\alpha,\sigma} \rangle$. For AFM order, one has $\mu_{A,\sigma} = \mu - \sigma h_s$, $\mu_{B,\sigma} = \mu + \sigma h_s$, and the condition $\Sigma_{B,\sigma}(\omega) = \Sigma_{A,-\sigma}(\omega)$. We consider spontaneously ordered solutions where the symmetry breaking fields vanish, $h_c, h_s \rightarrow 0$. The matrix elements of the local Green's function $\underline{G}(\omega)$ can be calculated by integrating the matrix elements of (3) over the density of states, which we choose as semi-elliptic, $\rho_0(\varepsilon) = 2\sqrt{D^2 - \varepsilon^2}/\pi D^2$. We solve the effective impurity problem with the numerical renormalization group [20, 21] (NRG) adapted to these cases with symmetry breaking. In these calculations we have chosen the discretization parameter $\Lambda = 1.8$ and we keep around 1000 states at each iterations. The initial bosonic Hilbert space is restricted to a maximum of 50 states. This is justified by the phonon occupation n_{ph} which does not exceed values of $n_{\text{ph}} \simeq 10$ except when λ is much larger than U .

In the AFM case the A -sublattice magnetization, $\Phi_{\text{afm}} = m_A = (n_{A,\uparrow} - n_{A,\downarrow})/2$ serves as an order parameter. For CO we define $\Phi_{\text{co}} = (n_A - 1)/2$. To identify the ground state of the system, we must compute the total ground state energy per lattice site, $E_{\text{tot}} = \langle H \rangle / N$, of the HH Hamiltonian (1) in the different phases. This gives generally,

$$E_{\text{tot}} = E_{\text{kin}} + E_U + E_{\text{ph}} + E_g. \quad (4)$$

The first term is the kinetic energy, which reads

$$E_{\text{kin}} = \sum_\sigma \int d\varepsilon_{\mathbf{k}} \rho_0(\varepsilon_{\mathbf{k}}) \varepsilon_{\mathbf{k}} \int d\omega f(\omega) \rho_{AB,\mathbf{k},\sigma}(\omega), \quad (5)$$

where $\rho_{AB,\mathbf{k},\sigma}(\omega) = -\text{Im}G_{AB,\mathbf{k},\sigma}(\omega)/\pi$ for the offdiagonal Green's function in (3) and $f(\omega)$ is the Fermi function. In the non-interacting case it can be evaluated analytically with $\rho_{\mathbf{k},\sigma}(\omega) = \delta(\omega - \varepsilon_{\mathbf{k}} + \mu)$, and we find for half filling, $\mu = 0$, $E_{\text{kin}}^0 = -4D/3\pi$, which for $D = 2$ is $E_{\text{kin}}^0 \simeq -0.8488$. This can be used as reference energy. The interaction energies E_U , E_g can be calculated from expectation values. We have

$$E_U = \frac{U}{2} \sum_\alpha \langle \hat{n}_{\alpha,\uparrow} \hat{n}_{\alpha,\downarrow} \rangle, \quad E_g = \frac{g}{2} \sum_\alpha \langle (b_\alpha + b_\alpha^\dagger)(\hat{n}_\alpha - 1) \rangle. \quad (6)$$

We distinguish between A - and B -sublattice values, which are equal in the AFM case, but not for the CO case. The third term for the total energy is generally given by the expectation value of the number of excited phonons, $E_{\text{ph}} = \omega_0 \langle b^\dagger b \rangle$. The detailed behavior of the various contributions to the energy in the different phases as well as static and dynamic response functions will be discussed elsewhere [22].

Results. – The half bandwidth $D = 2t = W/2$ is chosen as 2 in the following to set the energy scale. In Fig. 2 the phase diagram is shown for $\omega_0 = 0.6$ to exemplify the behavior neither too close to the adiabatic nor to the antiadiabatic regime. We carried out numerous calculations for other values of ω_0 and apart from the location of the point separating continuous and discontinuous transitions similar behavior was found for other choices. Notice that for physical optical phonons ($\omega_0 \sim 0.01W - 0.2W$) this value is rather large and the later presented results for $\omega_0 = 0.2$ can serve as a better guideline. Limiting cases of the phase diagram are known and easily understood on a qualitative level. Along the U -axis, the pure repulsive Hubbard model (at half filling on a bipartite lattice) is known to be AFM ordered at weak coupling [23], and this order is smoothly connected to the strong coupling Heisenberg AFM [24, 25]. Along the λ -axis, the pure Holstein model has a charge ordered ground state for $g > 0$ and $\omega_0 > 0$ [26], where the limits of weak and strong coupling are smoothly connected. For finite U and g we find that the transition line is approximately given by the line $\lambda \simeq U$. For the cases of weak and intermediate coupling ($U < W$) the order parameters become very small in our calculation close to the line $U_{\text{eff}} = 0$. An example is shown for fixed $U = 2$ in Fig. 3 (top), where the order parameters are plotted as a function of λ .

Near $\lambda = U$ the ordering scale is very small ($< 10^{-3}$) and can not be resolved well in our DMFT-NRG calculations, which then do not converge sufficiently well. The transition appears to be continuous, as all relevant response quantities change continuously. There are strong indications that it occurs directly from an ordered to an ordered state and no intermediate regime exists. We draw this conclusion by considering the behavior for different values of ω_0 (see also Fig. 4). For $n = 1$ in the antiadiabatic case, $\omega_0 \rightarrow \infty$, it is known that for any finite $U_{\text{eff}} > 0$ the system is AFM ordered [23] and for $U_{\text{eff}} < 0$ in the CO or SC state [27]. We have therefore a continuous transition from an ordered to an ordered state at $U_{\text{eff}} = 0$ on varying U or λ . In the DMFT-NRG calculations we find that the smaller ω_0 is the larger the order parameters near the transition become (see Fig. 4). Thus we conclude that this transition scenario persists for weak coupling and finite ω_0 . Mean field calculations in the adiabatic limit, $\omega_0 \rightarrow 0$, also support the picture of a direct transition between ordered states, however, the transition is discontinuous then. From NRG calculations in the normal state we can calculate a local effective quasiparticle interaction

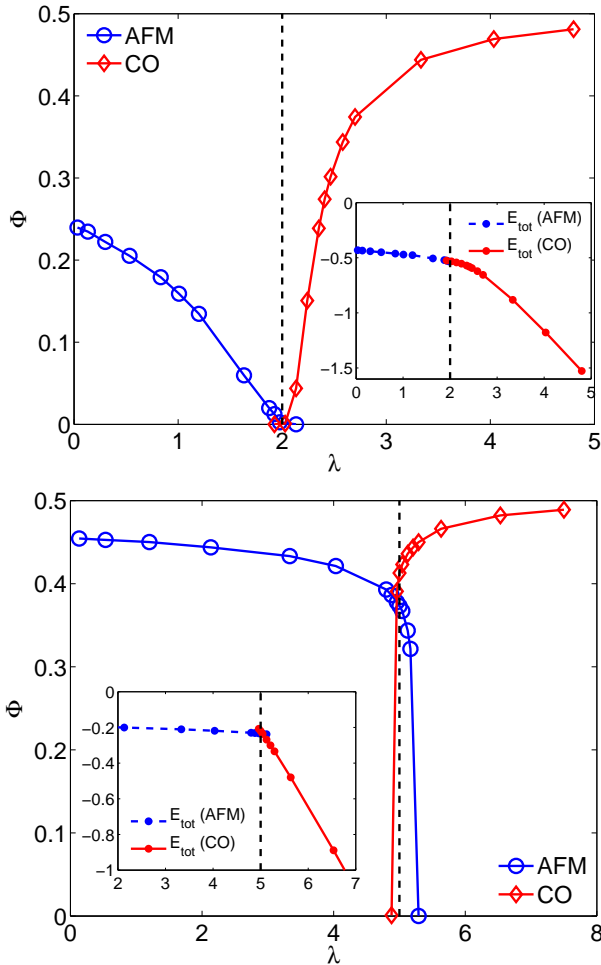


Fig. 3: (Color online) The expectation values Φ_{afm} and Φ_{co} for $U = 2$ (top) and $U = 5$ (bottom) as a function of λ . The total energy can be seen in the inset.

U^r by comparing the magnitude of the lowest two-particle excitation energy with twice the one-particle excitations energy at the fixed point [25]. U^r changes sign approximately at $U_{\text{eff}} = 0$, which is consistent with a change of ground states there. To examine in detail what happens exactly at the transition at weak coupling and to analyze the critical properties requires an effective theory specifically for this transition.

For larger couplings we have included in Fig. 2 a dashed line (\diamond) above which DMFT-NRG finds solutions with finite Φ_{co} and another one (\circ) below which Φ_{afm} is well finite. An example for this behavior is shown in Fig. 3 (bottom) for $U = 5$, where a much sharper behavior is seen. The calculation of the total ground state energy (see inset of Fig. 3) shows that also here the transition occurs approximately at $U_{\text{eff}} \simeq 0$. A number of quantities such as the double occupancy $\langle \hat{n}_{\uparrow} \hat{n}_{\downarrow} \rangle$ show discontinuities at the transition. The total energy is a continuous function of λ , but it displays a kink at the transition, such that a first derivatives will be discontinuous. The transition can be studied as a function of U for fixed λ , and a very similar picture emerges for weak and strong coupling. For details

we refer to [22].

As already alluded to, apart from the coupling strength the behavior near the transition also depends on the phonon frequency. In the adiabatic limit, $\omega_0 \rightarrow 0$, the phonons are represented by a static field, and one does not find a substantial modification of the ordered state as long as U_{eff} does not change sign. When this happens the order changes abruptly and we find a discontinuous transition. In the antiadiabatic limit we deal with an effective

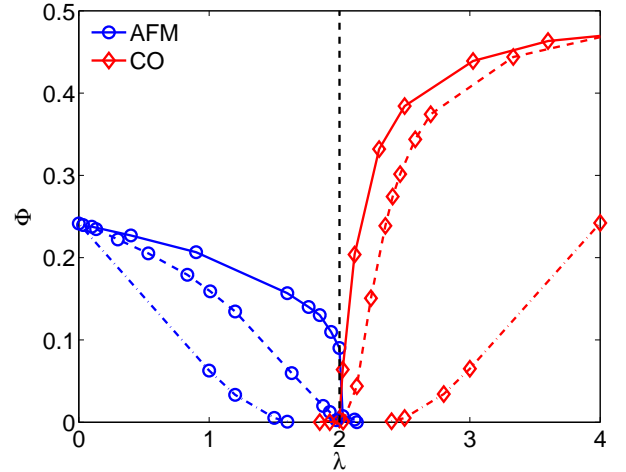


Fig. 4: (Color online) The expectation values Φ for fixed $U = 2$ varying λ . We show the results for $\omega_0 = 0.2$ (full line), $\omega_0 = 0.6$ (dashed line), and $\omega_0 \rightarrow \infty$ (dot-dashed line).

Hubbard model with U_{eff} . The bare coupling becomes very small close to the transition, where it changes sign. This gives then behavior of a renormalized mean field theory with an exponential behavior of the order parameter, which goes to zero for $U_{\text{eff}} \rightarrow 0$, and thus a continuous transition. Our calculations access the behavior between these limiting cases and we give examples for the behavior of Φ for fixed U and varying λ for $\omega_0 = 0.2, 0.6$ and $\omega_0 \rightarrow \infty$ in Fig. 4. We can see that the order for finite ω_0 is always larger than in the $\omega_0 \rightarrow \infty$ case. Our results give discontinuous transitions upon varying λ for $U \geq 4$ for $\omega_0 = 0.6$, whilst for $\omega_0 = 0.2$ already for $U \geq 3$.

More insight into the properties of the system are provided by the electronic spectral function. Here we consider the (majority) local lattice Green's function $G_{A,\uparrow}(\omega)$, which is given by the momentum sum of the diagonal element of (3), and its spectral function $\rho_{A,\uparrow}(\omega) = -\text{Im}G_{A,\uparrow}(\omega)/\pi$. $\rho_{\alpha,\sigma}(\omega)$ is symmetric at half filling in the normal state but becomes asymmetric in situations with symmetry breaking. Note that at half filling the spectra for minority spin in the AFM case, $\rho_{A,\downarrow}(\omega)$, and for the B -lattice for the charge order, $\rho_{B,\uparrow}(\omega)$, can be obtained from $\omega \rightarrow -\omega$. In Fig. 5 we show the spectral function for $U = 2$ and various values of λ approaching the transition in the AFM and CO state for $\omega_0 = 0.2$ and $\omega_0 = 0.6$. For comparison we have added the normal state spectral function for $U = \lambda$ as a dotted line in all cases.

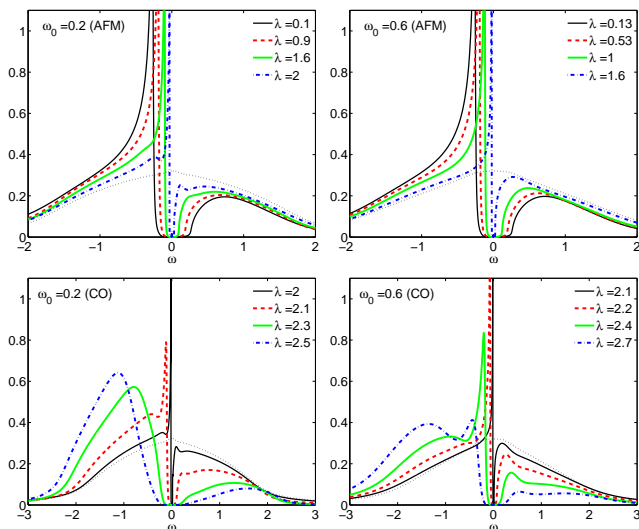


Fig. 5: (Color online) The local A -lattice (majority) spectral functions $\rho_{A,\uparrow}(\omega)$ in comparison AFM (upper part) and CO state (lower part) for $\omega_0 = 0.2, 0.6$ for fixed $U = 2$ and various λ approaching the transition. The dotted line gives the spectral function in the normal state without symmetry breaking for $U = \lambda$ for comparison.

In the AFM state for small λ , the spectra fit well to the mean field description, where a square root divergence is found below the gap and square root increase above the gap. [24] The higher energy parts are little modified for the case of $U = 2$ apart from the broadening of the band edges, but no features which can be attributed to the phonons can be identified. When interpreting the spectra one has to take into account the broadening and the limited energy resolution of the NRG at higher energies, which limit the accuracy. On increasing λ , the AFM order and magnitude of the spectral gap decreases. The electron phonon coupling is effective here in screening the repulsive U -term. No polaronic features can be identified in the spectra as the coupling is fairly weak. For $\omega_0 = 0.6$, the general form of the spectrum remains the same on increasing λ , whereas for $\omega_0 = 0.2$ small features near the gap emerge. In this case one can see that the ordered solution and spectral gap persist for values of λ up to $\sim U$, whilst for $\omega_0 = 0.6$ the gap vanishes earlier on increasing λ (see also Fig. 4 for Φ).

In the CO state close to the transition, $\lambda \geq U$, similar spectral characteristics of a weak coupling instability at the Fermi surface ($\omega = 0$) as in the AFM case can be seen both for $\omega_0 = 0.2$ and $\omega_0 = 0.6$. In the limit $\omega_0 \rightarrow \infty$ we would find very similar behavior in the CO state on increasing λ as in the AFM state on increasing U , but as illustrated around Eq. (2) the phonon-mediated attraction has an ω -dependent dynamic form, which leads to different behavior. One can identify a pronounced quasiparticle peak for interaction values near the transition which however becomes suppressed for larger values of λ . This suppression can be partly due to the broadening in the

NRG procedure as discussed in detail for superconducting solutions [28]. On increasing λ a principal peak develops in the CO spectrum. Its position, is fairly well described by the spectral shift of fully polarized mean field theory, $\Delta_{\text{mf}} = U n_{-\sigma}^A - 2\lambda\Phi_{\text{co}}$, for instance, $\Delta_{\text{mf}} = 1.5$ for $\lambda = 2.5$ and $U = 2$ (cf. CO spectrum for $\omega_0 = 0.2$).

We make a few general remarks concerning the phase diagram which has been established. It is remarkable that the phase diagram of the HH model in one dimension [9] is similar to Fig. 2. There one finds a Mott insulator with strong antiferromagnetic correlations, but *no* long range order, when $U_{\text{eff}} > 0$, and a Peierls, charge ordered, insulator for $U_{\text{eff}} < 0$. There is, however, a metallic region with finite spin gap, but no charge gap in between these two phases [8, 9, 11]. For larger U this intermediate region shrinks until one finds a direct first order Mott-Peierls transition, similar to the present observation. A major difference with the high dimensional results is the real symmetry breaking in our case as well as the existence of the intermediate region, for which we find no indication here.

We comment on the possible relevance of this work for the three dimensional compound $\text{Ba}_{1-x}\text{K}_x\text{BiO}_3$ bearing in mind that there are still controversial issues. According to band theory the compound would be metallic for $x = 0$ with a half filled Bi $6s$ band, but it shows CO [29] accompanied by a lattice distortion, which hints towards a strong coupling of the electrons to the lattice. For $x > 0.35$, SC with fairly high $T_c \approx 30$ K appears [29]. A strong coupling to an oxygen breathing mode at roughly 70meV is thought to play an important role [30, 31]. Thus, it has been proposed that the Holstein or HH model with effective bandwidth $W \approx 4\text{eV}$ can provide an approximate description of the compound and account for the prominent features of the phase diagram including CO and SC [32–34]. Estimates for the dimensionless electron-phonon coupling constant, denoted by $\bar{\lambda}$ here, based on density functional calculations vary substantially, $\bar{\lambda} = 0.4 - 1.5$ [31, 35–37]. If we take $\bar{\lambda} = \lambda\rho_0(0) \simeq 1$, such that $\lambda \simeq 3.14t$, then according to the phase diagram in Fig. 2 the experimentally observed CO state can be explained only if the residual local repulsion U is significantly less than $\lambda = 0.79W$. This is consistent with the estimates for a residual positive U in an effective one-band model $U/W \approx 0.2$ [38]. With the latter estimate for U even for $\bar{\lambda} = 0.4$ [37] a CO state is stable for $x = 0$. However, for such small $\bar{\lambda}$ it is difficult to explain the high T_c for superconductivity in the conventional theory. These issues, including appropriate values for $\bar{\lambda}$ for different fillings, still have to be clarified by future research. Once suitable values are found, the approach presented here or refinements of it can make predictions for quantities such as the spectral gap or the transition temperature for the CO and SC state.

A question raised in this work is why the transition between the two ordered states occurs for $U \simeq \lambda$ in such a generality. Both bare interactions produce opposite effects for the interactions of low energy quasiparticles. The fact

that the sign of the bare values $U - \lambda$ is reproduced for the effective quasiparticle interaction U^r suggests that U and g^2 are renormalized in the same way. A reason for this is the specific form of the electron-phonon coupling to the local density and the phase space restriction at half filling. This is different away from half filling and for couplings to other modes such as of the Jahn-Teller type [3]. A renormalization group study [10] has examined the competing interactions for the HH model in one dimension. Extensions to higher dimensions would be of great interest.

Conclusions. – We analyzed competing interaction effects and established the ground state phase diagram of the infinite dimensional Hubbard-Holstein model at half filling with a transition line $U \simeq \lambda$. This implies that unlike superconductivity, where retardation is effective, phonon induced CO prevails only if λ exceeds the Coulomb repulsion. However as seen in Fig. 3, a small excess can be sufficient to have a strongly ordered state. We also identified a point separating continuous and discontinuous transitions. A continuous quantum phase transition between different ordered state is rare and could be of interest for further study. We expect the presented phase diagram to be general as it holds for finite ω_0 as well as in the adiabatic and antiadiabatic limiting cases. From the similarities with the one-dimensional phase diagram, and recent results in $d = 2$ [39] (adiabatic limit), we conjecture that the form of the phase diagram possesses validity also in two and three dimensions. Extensions to finite temperature and other fillings would be desirable, where the competition can be studied in the case of superconductivity.

I wish to thank O. Gunnarsson, A.C. Hewson, G. Sangiovanni, and R. Zeyher for helpful discussions, and W. Koller and D. Meyer for their earlier contributions to the development of the NRG programs.

REFERENCES

- [1] MOREL P. and ANDERSON P. W., *Phys. Rev.* , **125** (1962) 1263.
- [2] LANZARA A., BOGDANOV P. V., ZHOU X. J., KELLER S. A., FENG D. L., LU E. D., YOSHIDA T., EISAKI H., FUJIMORI A., KISHIO K., SHIMOYAMA J.-I., UCHIDA T. N. S., HUSSAIN Z. and SHEN Z.-X., *Nature* , **412** (2001) 510.
- [3] GUNNARSON O., *Alkali-Doped Fullerenes: Narrow-Band Solids with Unusual Properties* (World Scientific, Singapore) 2004.
- [4] MILLIS A. J., *Nature* , **392** (1998) 147.
- [5] POWELL B. and MCKENZIE R. H., *J. Phys.: Cond. Mat.* , **18** (2006) 827.
- [6] HUBBARD J., *Proc. R. Soc. London, Ser. A* , **276** (1963) 238.
- [7] HOLSTEIN T., *Ann. Phys. (N.Y.)* , **8** (1959) 325.
- [8] CLAY R. T. and HARDIKAR R. P., *Phys. Rev. Lett.* , **95** (2005) 096401.
- [9] HARDIKAR R. P. and CLAY R. T., *Phys. Rev. B* , **75** (2007) 245103.
- [10] TAM K.-M., TSAI S.-W., CAMPBELL D. K. and CASTRO NETO A. H., *Phys. Rev. B* , **75** (2007) 161103.
- [11] H. FEHSKE G. H. and JECKELMANN E., *Europhys. Lett.* , **84** (2008) 57001.
- [12] GEORGES A., KOTLIAR G., KRAUTH W. and ROZENBERG M., *Rev. Mod. Phys.* , **68** (1996) 13.
- [13] JEON G. S., PARK T.-H., HAN J. H., LEE H. C. and CHOI H.-Y., *Phys. Rev. B* , **70** (2004) 125114.
- [14] KOLLER W., MEYER D., ONO Y. and HEWSON A. C., *Europhys. Lett.* , **66** (2004) 559.
- [15] KOLLER W., MEYER D. and HEWSON A. C., *Phys. Rev. B* , **70** (2004) 155103.
- [16] KOLLER W., HEWSON A. C. and EDWARDS D. M., *Phys. Rev. Lett.* , **95** (2005) 256401.
- [17] SANGIOVANNI G., CAPONE M., CASTELLANI C. and GRILLI M., *Phys. Rev. Lett.* , **94** (2005) 026401.
- [18] SANGIOVANNI G., GUNNARSSON O., KOCH E., CASTELLANI C. and CAPONE M., *Phys. Rev. Lett.* , **97** (2006) 046404.
- [19] METZNER W. and VOLLHARDT D., *Phys. Rev. Lett.* , **62** (1989) 324.
- [20] WILSON K., *Rev. Mod. Phys.* , **47** (1975) 773.
- [21] BULLA R., COSTI T. and PRUSCHKE T., *Rev. Mod. Phys.* , **80** (2008) 395.
- [22] BAUER J. and HEWSON A. C., to be published (2010).
- [23] VAN DONGEN P. G. J., *Phys. Rev. Lett.* , **67** (1991) 757.
- [24] ZITZLER R., PRUSCHKE T. and BULLA R., *Eur. Phys. J. B* , **27** (2002) 473.
- [25] BAUER J. and HEWSON A. C., *Eur. Phys. J. B* , **57** (2007) 235.
- [26] FREERICKS J. K., JARRELL M. and SCALAPINO D. J., *Phys. Rev. B* , **48** (1993) 6302.
- [27] MICNAS R., RANNINGER J. and S.ROBASZKIEWICZ, *Rev. Mod. Phys.* , **62** (1990) 113.
- [28] BAUER J., HEWSON A. C. and DUPUIS N., *Phys. Rev. B* , **79** (2009) 214518.
- [29] HINKS D. G., DABROWSKI B., RICHARDS D. R., JORGENSEN J. D., PEI S. and ZASADZINSKI J. F., *Physica C: Superconductivity* , **162-164** (1989) 1405 .
- [30] LOONG C.-K., VASHISHTA P., KALIA R. K., DEGANI M. H., PRICE D. L., JORGENSEN J. D., HINKS D. G., DABROWSKI B., MITCHELL A. W., RICHARDS D. R. and ZHENG Y., *Phys. Rev. Lett.* , **62** (1989) 2628.
- [31] CHAINANI A., YOKOYA T., KISS T., SHIN S., NISHIO T. and UWE H., *Phys. Rev. B* , **64** (2001) 180509.
- [32] VEKIĆ M., NOACK R. M. and WHITE S. R., *Phys. Rev. B* , **46** (1992) 271.
- [33] FREERICKS J. K., *Phys. Rev. B* , **50** (1994) 403.
- [34] BERGER E., VALÁŠEK P. and VON DER LINDEN W., *Phys. Rev. B* , **52** (1995) 4806.
- [35] SHIRAI M., SUZUKI N. and MOTIZUKI K., *J. Phys.: Cond. Mat.* , **2** (1990) 3553.
- [36] LIECHTENSTEIN A. I., MAZIN I. I., RODRIGUEZ C. O., JEPSEN O., ANDERSEN O. K. and METHFESSEL M., *Phys. Rev. B* , **44** (1991) 5388.
- [37] MEREGALLI V. and SAVRASOV S. Y., *Phys. Rev. B* , **57** (1998) 14453.
- [38] VIELSACK G. and WEBER W., *Phys. Rev. B* , **54** (1996) 6614.
- [39] KUMAR S. and VAN DEN BRINK J., *Phys. Rev. B* , **78** (2008) 155123.